Available online at www.sciencedirect.com
SCIENCE DIRECT®
Journal of Sound and Vibration 272 (2004) 471–493
JOURNAL OF SOUND AND VIBRATION
www.elsevier.com/locate/jsvi

Extracting bridge frequencies from the dynamic response of a passing vehicle

Y.-B. Yang[a,*], C.W. Lin[a], J.D. Yau[b]

[a] *Department of Civil Engineering, National Taiwan University, No. 1, Sec 4, Roosevelt Road, Taipei 10617, Taiwan*
[b] *Department of Architecture & Building Technology, Tamkang University, Taipei 10620, Taiwan*

Received 9 September 2002; accepted 26 March 2003

Abstract

The frequencies of vibration of bridges represent a kind of information that is most useful for many purposes. Traditional vibration tests aimed at measuring the bridge frequencies often require on-site installation of the measurement equipment, which is not only costly, but also inconvenient. As a first attempt, the idea of using a vehicle moving over a bridge as a *message carrier* of the dynamic properties of the bridge is theoretically explored in this paper. In order to *identify* the key parameters dominating the vehicle–bridge interaction response, while *illustrating* the key phenomena involved, assumptions that lead to closed-form solutions are adopted in the analytical study. For instance, a vehicle is modelled as a sprung mass, and a bridge as a simply supported beam considering only the first mode of vibration. The concept of extracting bridge frequencies from a passing vehicle, however, is *not* restricted by the aforementioned assumptions, as will be demonstrated in an independent finite element study, which do not rely on any particular assumptions. Concluding remarks are given concerning the *feasibility* of extracting the bridge frequencies from the dynamic response of a passing vehicle, along with directions for future research identified.

1. Introduction

The measurement of the frequencies of vibration of a bridge, especially the one of the fundamental mode, is a problem widely encountered in bridge engineering. When a new bridge is completed, one is interested in the frequencies of vibration, at least the first few ones, since they serve as useful parameters for comparison with those predicted by the numerical model. How well the measured frequencies agree with the predicted ones is an indication of the appropriateness of

*Corresponding author. Tel.: +886-2-2363-2104; fax: +886-2-2363-7585.
E-mail address: ybyang@ntu.edu.tw (Y.-B. Yang).

0022-460X/03/$ - see front matter
doi:10.1016/S0022-460X(03)00378-X

the model used in analysis and design. Such information provides useful clues for calibrating models used in related designs, concerning the uncertainties in material properties, structural connectivity and boundary conditions. For the purpose of maintenance or rehabilitation, it is often required that the frequencies of vibration of the bridge be measured, in addition to the damping or other dynamic properties. In this regard, the frequencies of vibration, when monitored over a long period, serve as a useful reference for evaluating the degradation in stiffness or strength of the structure, and even for identifying possible damages in the structure, say, due to long-term overloading and impacts by heavy trucks or earthquake tremors.

Traditionally, the measurement of the frequencies of a bridge requires some on-site instrumentation, which may be costly, time-consuming, and even dangerous, depending on the location and type of bridges. One common practice is to mount the vibration sensors, such as seismometers, at different positions of the bridge and have them connected to a PC-driven data acquisition system. For the case where the on-going traffic cannot be partially terminated for the purpose of experimentation, the task of equipment mounting and data acquisition is generally risky. Nevertheless, the on-going traffic can continuously input a certain amount of energy to the bridge, usually large enough to excite the higher modes of vibration. Researches conducted along this line, utilizing the on-going traffic or controlled vehicular excitations as the source of excitation, include McLamore et al. [1], Abdel-Ghaffar et al. [2], Mazurek and DeWolf [3], Casas [4], Paultre et al. [5], Ventura et al. [6], Conner et al. [7], and Farrar and James III [8], among others.

For the case where the traffic can be temporarily terminated for experiment or before a bridge is opened to the traffic, either an ambient vibration test (in the sense of no on-going traffic in this paper), an impact test or a forced vibration test can be conducted on the bridge. In the ambient vibration test, the frequencies of vibration of the bridge are measured with the bridge remaining basically not excited by any artificial force [8–10]. For this reason, such tests may not yield results with high amplitudes for the bridge frequencies, especially of the higher modes, due to the involvement of environmental noises. For structures that are susceptible to wind loads, such as the cable-stayed and suspension bridges, field measurements showing rather high peaks for the first several frequencies were conducted by researchers for wind-induced vibrations [11,12]. In the impact test, the bridge is excited by an impulse or impact force generated by devices such as heavy hammers or by letting the rear wheels of a truck drop from a wooden block. The level of impact forces is usually large enough to excite the first several modes [13,14]. An alternative is to conduct a forced vibration test on the bridge, using devices such as the vibration shaker [8,9,15,16]. This method allows us to identify the first few frequencies of vibration, as the input energy is usually large enough to meet such a need.

Although the techniques for conducting the aforementioned tests are generally mature, the effort, i.e., time, cost and manpower, required in conducting each test is considerable. The objective of this paper is to explore the *feasibility* of extracting the frequencies of vibration of a bridge, at least the fundamental one, from the dynamic response of a vehicle passing the bridge. The idea is that a vehicle passing a bridge with a specific speed can excite the bridge to a certain level, thereby playing the role of a *vibration shaker*. The vehicle in the meantime functions like a *moving sprung mass*, whose dynamic response is affected by the dynamic properties of the supporting bridge. Thus, if we can record the vertical dynamic (acceleration) response of the vehicle during its passage of the bridge using seismometers installed inside the vehicle, we can

analyze the frequency content of that response, eliminating those frequencies related to the vehicle itself, and obtain frequencies associated with the supporting bridge.

There exists great academic interest to exploit the feasibility of extracting the bridge frequencies from a passing vehicle, as it was not attempted before, and in this regard it is essential to start with the first frequency in a *preliminary, theoretical* study, which forms the objective of this paper. In order to identify the key parameters dominating the vehicle–bridge interaction (VBI) response, while illustrating the key phenomena involved, assumptions that lead to closed-form solutions are adopted in the analytical study. In this regard, the vehicle is modelled as a sprung mass and the bridge as a simply supported beam considering only the first mode of vibration. However, in the parallel, independent finite element analysis, virtually all the assumptions made in the analytical study are either lessened or removed. Noteworthy is the fact that the key phenomena observed in the simplified analytical study can find their counterpart in the finite element study.

2. Formulation of the analytical theory

Fig. 1 shows a vehicle of speed v, modelled as a lumped mass m_v supported on a spring of stiffness k_v, moving across a simply supported bridge of length L with smooth pavement. If the effect of damping of the bridge is ignored, the equations of motion for the sprung mass and the bridge can be written as

$$m_v\ddot{q}_v + k_v(q_v - u|_{x=vt}) = 0, \tag{1}$$

$$m\ddot{u} + EIu'''' = f_c(t)\delta(x - vt), \tag{2}$$

where q_v denotes the vertical deflection of the sprung mass, δ is a delta function, a dot and a prime, respectively, denote differentiation with respect to time t and co-ordinate x of the beam, and E denotes the elastic modulus, I the moment of inertia, $u(x,t)$ the displacement, and m the mass per unit length of the beam. The contact force f_c existing between the sprung mass and the beam can be expressed as

$$f_c(t) = k_v(q_v - u|_{x=vt}) + m_v g, \tag{3}$$

where g is the acceleration of gravity. It should be noted that the vehicle displacement q_v is measured from the static equilibrium position of the vehicle. Because of this, no gravity term appears in Eq. (1). In contrast, the motion of the beam may be affected by the gravity load of the vehicle mass, as implied by the contact force f_c in Eq. (3).

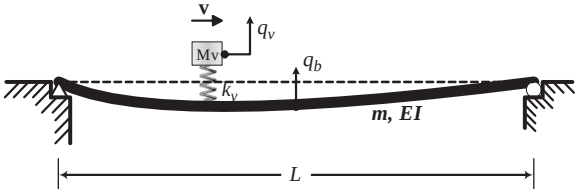

Fig. 1. Sprung mass moving over a beam.

For a moving load problem, which is transient in nature, the response of the beam can be well simulated by considering only the first mode of vibration [17]. In accordance, the displacement $u(x,t)$ of the beam can be approximated as

$$u(x,t) = q_b(t)\ \sin\left(\frac{\pi x}{L}\right), \tag{4}$$

where $q_b(t)$ denotes the generalized co-ordinate (or the midspan displacement) of the first mode for the beam. Substituting the preceding expression for u into Eqs. (1) and (2), multiplying both sides of Eq. (2) by $\sin(\pi x/L)$ and integrating with respect to length L of the beam, one obtains

$$m_v\ddot{q}_v + (\omega_v^2 m_v)q_v - \left[\omega_v^2 m_v \sin\left(\frac{\pi v t}{L}\right)\right]q_b = 0, \tag{5}$$

$$\frac{mL}{2}\ddot{q}_b + \left[\frac{mL}{2}\omega_b^2 + \omega_v^2 m_v \sin^2\left(\frac{\pi v t}{L}\right)\right]q_b - \left[\omega_v^2 m_v \sin\left(\frac{\pi v t}{L}\right)\right]q_v = -m_v g \sin\left(\frac{\pi v t}{L}\right), \tag{6}$$

where ω_v and ω_b denote the vibration frequency of the vehicle and the bridge, respectively,

$$\omega_v = \sqrt{\frac{k_v}{m_v}},\quad \omega_b = \frac{\pi^2}{L^2}\sqrt{\frac{EI}{m}}. \tag{7}$$

In the following, approximate closed-form solutions will be sought for the vehicle and bridge based on some practical assumptions.

3. Single-mode analytical solution

Assuming that the vehicle mass m_v has an order of magnitude much less than the bridge mass mL, i.e. $m_v/mL \ll 1$, one can approximate Eq. (6) by the following

$$\ddot{q}_b + \omega_b^2 q_b = \frac{-2m_v g}{mL}\sin\left(\frac{\pi v t}{L}\right). \tag{8}$$

By the use of zero initial conditions, one can obtain from the preceding equation the generalized co-ordinate q_b of the bridge as

$$q_b = \frac{\Delta_{st}}{1-S^2}\left[\sin\left(\frac{\pi v t}{L}\right) - S\sin(\omega_b t)\right], \tag{9}$$

where Δ_{st}, as given below, denotes approximately the static deflection of the midspan of the beam under the gravity action of the mass m_v at the same point

$$\Delta_{st} = -\frac{2m_v g L^3}{\pi^4 EI}, \tag{10}$$

which is very close to the exact value of $-m_v g L^3/(48EI)$. The speed parameter S is defined as the ratio of half the driving frequency $\pi v/L$ to the bridge frequency ω_b, i.e.,

$$S = \frac{\pi v}{L\omega_b}. \tag{11}$$

Substituting Eq. (9) for the bridge co-ordinate q_b into Eq. (5), one can solve from Eq. (5) the vehicle response q_v by Duhamel's integral as

$$q_v(t) = \frac{\omega_v \Delta_{st}}{2(1-S^2)}\left\{\frac{1}{\omega_v}(1-\cos\omega_v t) - \frac{\omega_v\left(\cos\left(2\pi v t/L\right) - \cos\left(\omega_v t\right)\right)}{\omega_v^2 - \left(2\pi v/L\right)^2}\right.$$
$$\left. -S\left[\frac{\omega_v\left(\cos\left(\left((\pi v/L)-\omega_b\right)t\right) - \cos\left(\omega_v t\right)\right)}{\omega_v^2 - \left((\pi v/L)-\omega_b\right)^2} - \frac{\omega_v\left(\cos\left(\left((\pi v/l)+\omega_b\right)t\right) - \cos\left(\omega_v t\right)\right)}{\omega_v^2 - \left((\pi v/L)+\omega_b\right)^2}\right]\right\}. \quad (12)$$

Evidently, the vehicle response is dominated by four specific frequencies, that is, the vehicle frequency, ω_v, driving frequency of the moving vehicle, $2\pi v/L$, and two shifted frequencies of the bridge, $\omega_b - \pi v/L$, $\omega_b + \pi v/L$. By letting μ denote the frequency ratio of the bridge to the vehicle, i.e., $\mu = \omega_b/\omega_v$, and by using the definition for the speed parameter S, i.e., $S = \pi v/(L\omega_b)$, one can rewrite the preceding equation as

$$q_v(t) = \frac{\Delta_{st}}{2(1-S^2)}\left[(1-\cos\omega_v t) - \frac{\cos 2\pi v t/L - \cos\omega_v t}{1-(2\mu S)^2} - S\frac{\cos\left(\omega_b - \pi v/L\right)t - \cos\omega_v t}{1-\mu^2(1-S)^2}\right.$$
$$\left. +S\frac{\cos\left(\omega_b + \pi v/L\right)t - \cos\omega_v t}{1-\mu^2(1+S)^2}\right], \quad (13)$$

which can be differentiated once to yield the velocity of the vehicle as

$$\dot{q}_v(t) = \frac{\Delta_{st}\omega_v}{2(1-S^2)}\left[\sin\omega_v t + \frac{2\mu S\sin 2\pi v t/L - \sin\omega_v t}{1-(2\mu S)^2} + S\frac{\mu(1-S)\sin\left(\omega_b - \pi v/L\right)t - \sin\omega_v t}{1-\mu^2(1-S)^2}\right.$$
$$\left. -S\frac{\mu(1+S)\sin\left(\omega_b + \pi v/L\right)t - \sin\omega_v t}{1-\mu^2(1+S)^2}\right], \quad (14)$$

and twice to yield the acceleration of the vehicle as

$$\ddot{q}_v(t) = \frac{\Delta_{st}\omega_v^2}{2(1-S^2)}\left[\cos\omega_v t + \frac{(2\mu S)^2\cos 2\pi v t/L - \cos\omega_v t}{1-(2\mu S)^2} + S\frac{\mu^2(1-S)^2\cos\left(\omega_b - \pi v/L\right)t - \cos\omega_v t}{1-\mu^2(1-S)^2}\right.$$
$$\left. -S\frac{\mu^2(1+S)^2\cos\left(\omega_b + \pi v/L\right)t - \cos\omega_v t}{1-\mu^2(1+S)^2}\right]. \quad (15)$$

Apparently, the vertical displacement, velocity and acceleration of the vehicle depend on both the parameters S and μ. In contrast, the central displacement of the bridge, as given in Eq. (9), depends only on the speed parameter S.

The maximum displacement response of the vehicle has been drawn with relation to the two parameters S and μ using a tri-phase plot in Fig. 2(a), of which the contour projection on the horizontal plane was given in Fig. 2(b). As can be seen, the vehicle achieves its maximum in the region with $S = 0.3-0.6$ and $\mu = 0.5-1.5$, especially in the vicinity of $\mu = 1$. This can be easily conceived, if one realizes that for $\mu = 1$, i.e., when the vehicle frequency approaches the bridge frequency, resonance will occur on the vehicle–bridge system, under which condition a significant amount of kinetic energy will be transmitted to the vehicle, a smaller subsystem compared with the bridge. For the purpose of extracting the bridge frequency from the vehicle response, it is preferable that the vehicle response be enlarged as much as possible, or if the peak regions noted above can be reached.

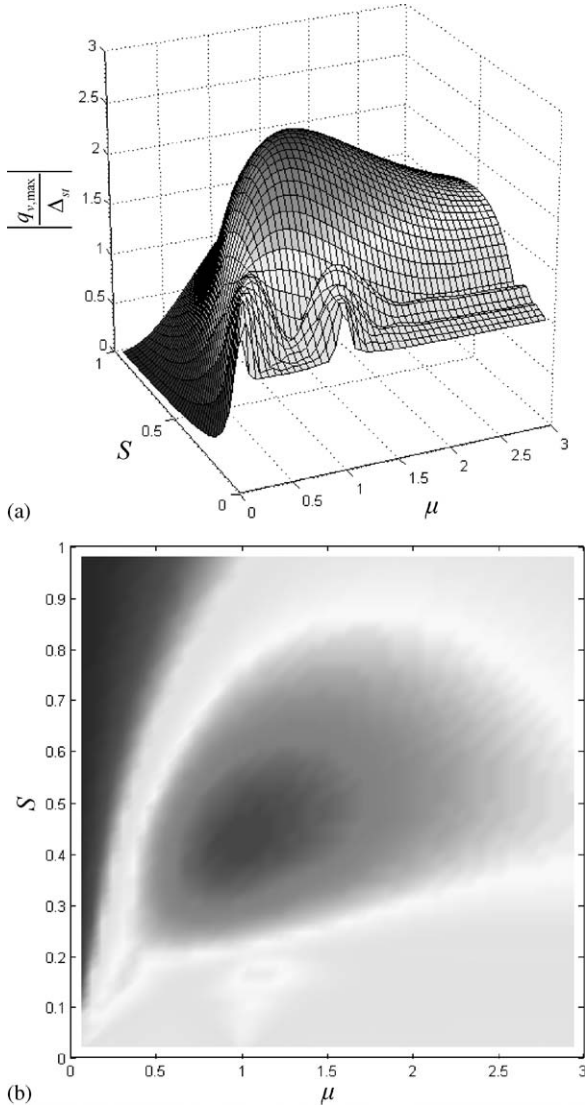

Fig. 2. Maximum displacement response of vehicle: (a) tri-phase plot and (b) plane projection.

Similarly, Figs. 3(a) and (b) show the tri-phase plot and contour lines, respectively, for the vertical velocity of the vehicle. Clearly, the maximum response of the vehicle velocity occurs in the region with $S = 0.3-0.6$ and $\mu = 0.5-1.0$ and in the vicinity of the point with $S = 0.3$ and $\mu = 1.0$. In addition, Figs. 4(a) and (b) show the tri-phase plot and contour lines, respectively, for the vehicle acceleration, which indicates that the maximum response occurs in two regions indicated by ($S = 0.3-0.4$, $\mu = 0.55-1.5$) and ($S = 0.3-0.5$, $\mu = 0-0.5$); the latter, however, can hardly be reached in practice.

As was mentioned above, in extracting the bridge frequency from the vehicle response, higher visibility can be achieved if the vehicle response can be magnified as much as possible. The above

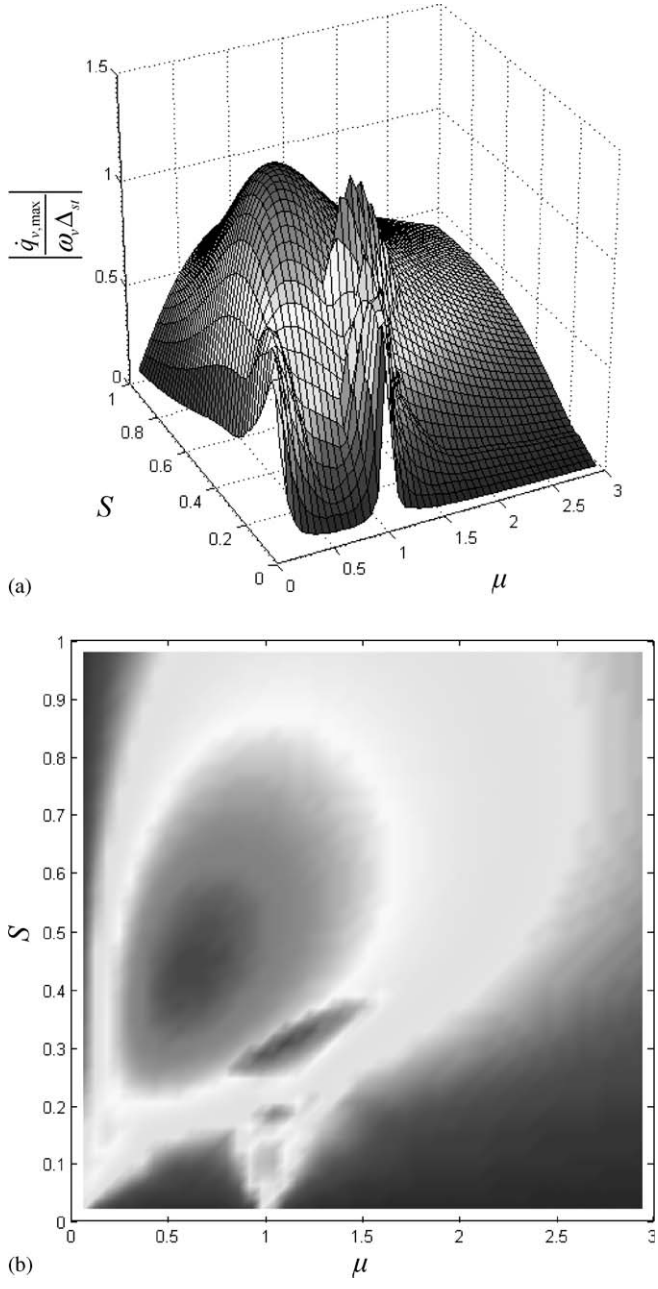

Fig. 3. Maximum velocity response of vehicle: (a) tri-phase plot and (b) plane projection.

analyses offer some clues for selecting the related physical parameters of the sprung mass in practice. In the following, we shall investigate the relative influence of each of four specific frequencies on the response amplitude of the vehicle. To this end, one may rewrite the vehicle

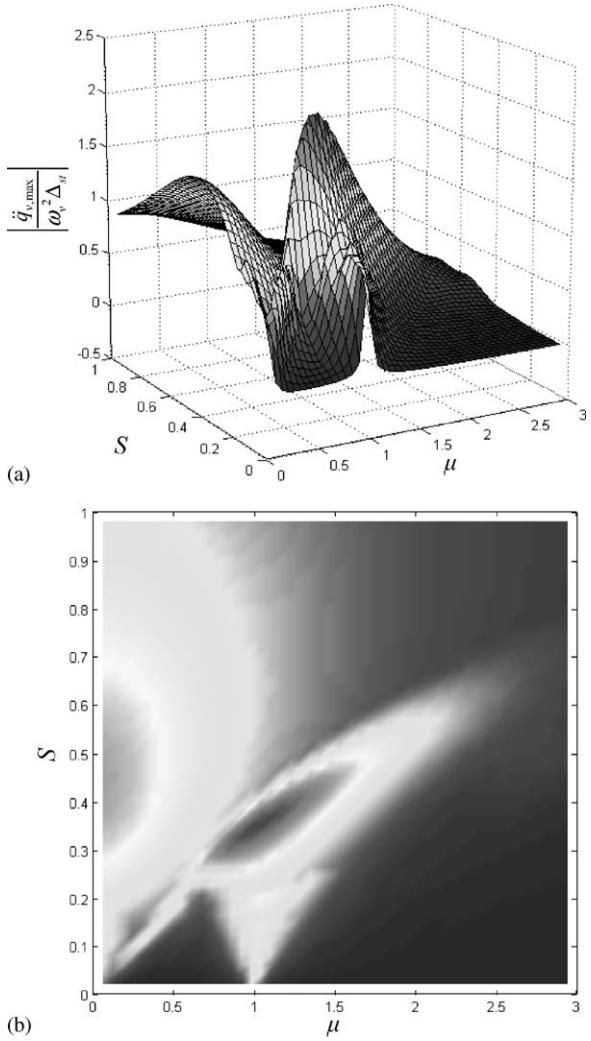

Fig. 4. Maximum acceleration response of vehicle: (a) tri-phase plot and (b) plane projection.

acceleration $\ddot{q}_v(t)$ as follows

$$\ddot{q}_v(t) = \frac{\Delta_{st}\omega_v^2}{2(1-S^2)}\left[A_1 \cos \omega_v t + A_2 \cos\frac{2\pi v}{L} + A_3 \cos\left(\omega_b - \frac{\pi v}{L}\right) + A_4 \cos\left(\omega_b + \frac{\pi v}{L}\right)\right], \quad (16)$$

where A_1, A_2, A_3, A_4 denote the relative magnitude of the contribution associated with each of the four frequencies,

$$A_1 = 1 - \frac{1}{1-(2\mu S)^2} - \frac{S}{1-\mu^2(1-S)^2} + \frac{S}{1-\mu^2(1+S)^2}, \qquad A_2 = \frac{(2\mu S)^2}{1-(2\mu S)^2}$$
$$A_3 = \frac{S\mu^2(1-S)^2}{1-\mu^2(1-S)^2}, \qquad A_4 = -\frac{S\mu^2(1+S)^2}{1-\mu^2(1+S)^2} \quad (17)$$

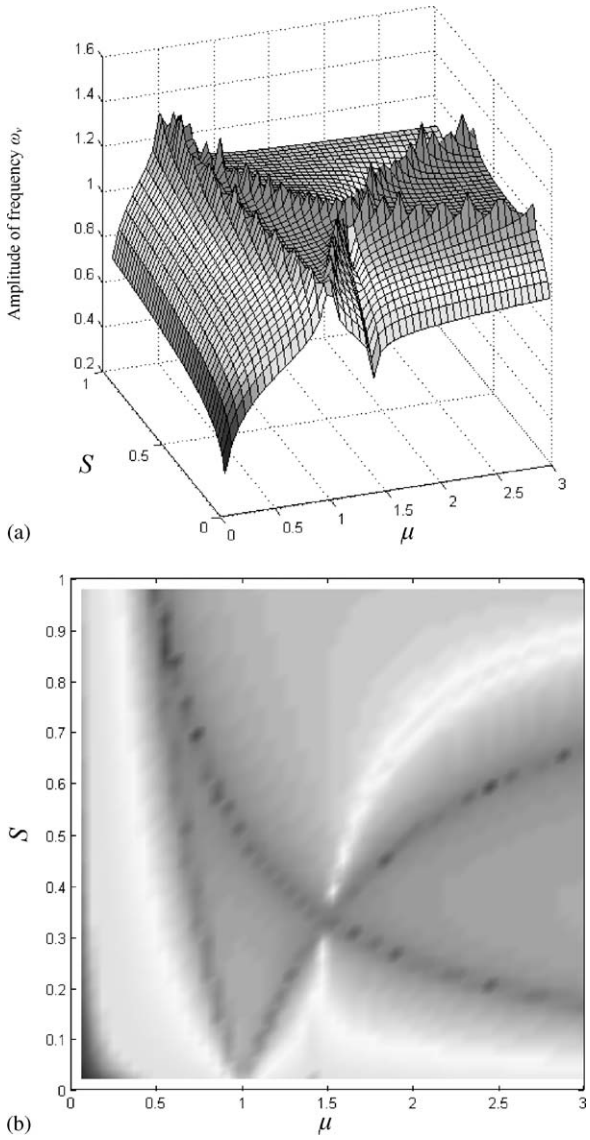

Fig. 5. Amplitude of frequency ω_v: (a) tri-phase plot and (b) plane projection.

In Figs. 5–8, the amplitude given in Eq. (17) associated with each of the four major frequencies has been plotted with respect to the speed parameter S and frequency ratio μ, along with the contour lines. Using the field data collected in Ref. [18], it can be shown that the maximum speed parameter S encountered in practice is no greater than 0.3. In contrast, a wider range exists for the frequency ratio μ, which is assumed to be from 0 to 3 in this study. For the range of parametric values considered, it can be observed that the term A_4 remains the largest among the four coefficients in Eq. (17), meaning that the peak response of the vehicle is dominated mainly by the term associated with the rightward shifted frequency of the bridge, i.e., $\omega_b + \pi v/L$.

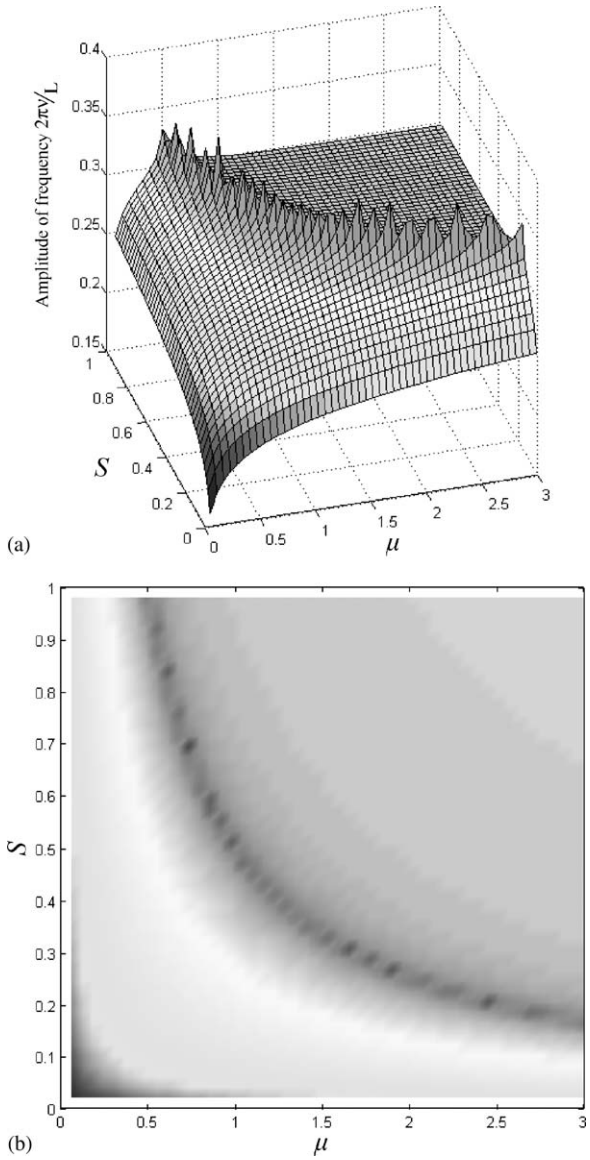

Fig. 6. Amplitude of frequency $2\pi v/L$: (a) tri-phase plot and (b) plane projection.

4. Conditions of resonance

In this paper, the condition of resonance is defined such that any of the denominators in the vehicle response equals zero. Under such a condition, the amplitude of the vehicle response reaches a local maximum or a local peak in the frequency response plot. As can be seen from Eq. (12), four conditions of resonance can occur on the VBI system, as will be described below.

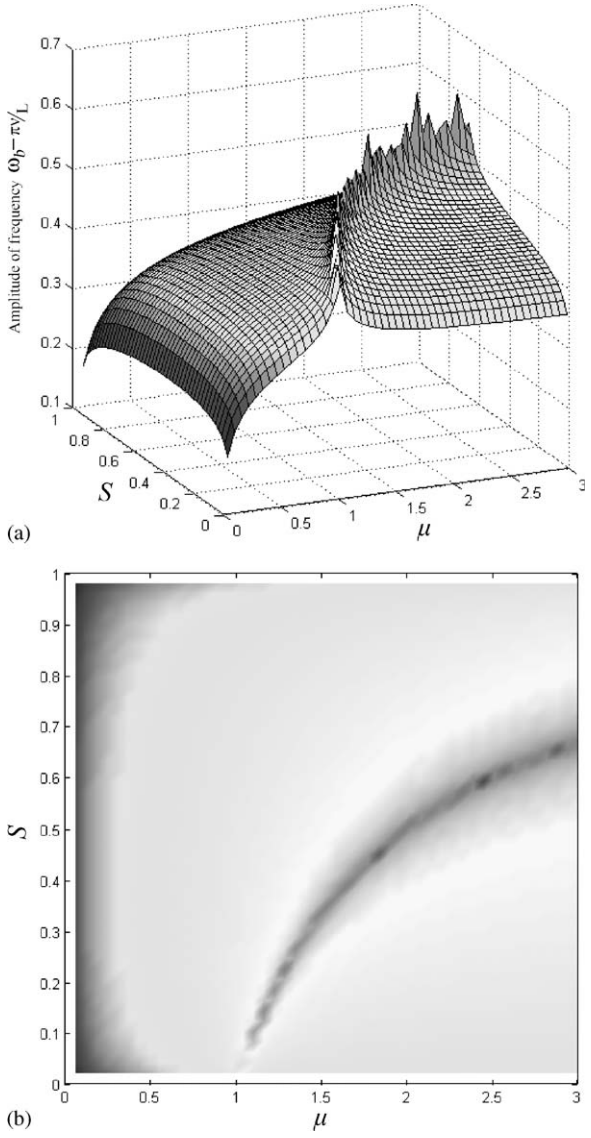

Fig. 7. Amplitude of frequency $\omega_b - \pi v/L$: (a) tri-phase plot and (b) plane projection.

The first condition occurs when $S = 1$, which implies that half the driving frequency of the vehicle, $\pi v/L$, equals the fundamental frequency ω_b of the bridge, according to Eq. (11). Such a condition can hardly be met in practice, as it implies an unreasonably high vehicle speed.

The second condition occurs when, $\omega_v^2 - (2\pi v/L)^2 = 0$ which can be further split into two as $\omega_v + 2\pi v/L = 0$ and $\omega_v - 2\pi v/L = 0$. The former can never be met mathematically. The latter can be rewritten as $T_v = L/v$, meaning that the time required for the vehicle to pass the bridge, L/v, must equal the period T_v of the vehicle. For a vehicle with a vibration period of $T_v = 1-0.3$ s

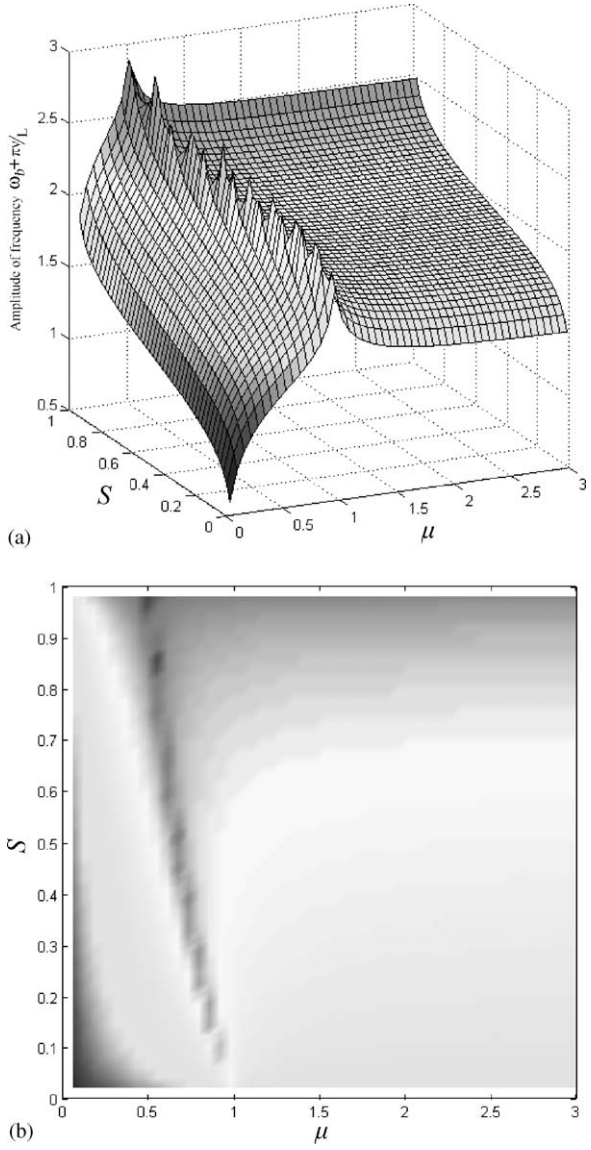

Fig. 8. Amplitude of frequency $\omega_b + \pi v/L$: (a) tri-phase plot and (b) plane projection.

passing a bridge, say, of length $L = 30$ m, the vehicle speed v must be in the range of 30–90 m/s (or 108–324 km/h), in order to excite the condition of resonance, which can hardly be met in practice.

The third condition occurs when $\omega_v^2 - \left(\pi v/L - \omega_b\right)^2 = 0$, which can be factored as $\omega_v + \left(\omega_b - \pi v/L\right) = 0$ and $\omega_v - \left(\omega_b - \pi v/L\right) = 0$. The former cannot be met in practice, since half the driving frequency, $\pi v/L$, is generally smaller than the bridge frequency ω_b. The latter condition can be possibly met, if the bridge frequency ω_b happens to be slightly larger than the vehicle frequency ω_v.

The fourth condition occurs when $\omega_v^2 - (\pi v/L + \omega_b)^2 = 0$, which can be factored as $\omega_v + (\omega_b + \pi v/L) = 0$ and $\omega_v - (\omega_b + \pi v/L) = 0$. The former can never be met mathematically. The latter condition can be possibly met, if the bridge frequency ω_b happens to be slightly smaller than the vehicle frequency ω_v.

From the above analysis, it is concluded that if the bridge frequency ω_b is close to the vehicle frequency ω_v, then the vehicle can be excited to resonance through adjustment of the vehicle speed v, such that either of the following two conditions are met: $\omega_v - (\omega_b - \pi v/L) = 0$ and $\omega_v - (\omega_b + \pi v/L) = 0$, as will be demonstrated in the numerical study. Moreover, the vehicle response is dominated by the four specific frequencies: ω_v, $2\pi v/L$, $\omega_b - \pi v/L$, and $\omega_b + \pi v/L$, using the present single-mode approximation.

5. Simulation by the finite element method

The above analytical study, though unavoidably based on some assumptions, serves to identify the key parameters dominating the VBI response. They serve as guidelines for simulating the same problem using more sophisticated or realistic approaches, say, the finite element method or experimental means. In fact, the idea of extracting bridge frequencies from the vehicle response is *not restricted* by any of the assumptions adopted in the analytical study, since the bridge frequencies, by nature, are always implied in the response of vehicles traveling over the bridge, as will be demonstrated in the finite element simulation to follow, for which most assumptions will be removed. The main question in developing the technology is *how to extract or interpret* the bridge frequencies from the response "measured" (as in the field test) or "calculated" (as in this pilot study) for the passing vehicle.

For the present purposes, let us discretize the beam into a number of elements and assume the sprung mass to be acting at only one of the elements. The equations of motion for the sprung mass m_v and the bridge element directly in contact can be written as [19]

$$\begin{bmatrix} m_v & 0 \\ 0 & [m_b] \end{bmatrix} \begin{Bmatrix} \ddot{q}_v \\ \{\ddot{u}_b\} \end{Bmatrix} + \begin{bmatrix} c_v & -c_v\{N\}^{\mathrm{T}} \\ -c_v\{N\} & [c_b] + 2vm_v\{N\}\dfrac{\partial\{N\}^{\mathrm{T}}}{\partial x} + c_v\{N\}\{N\}^{\mathrm{T}} \end{bmatrix} \begin{Bmatrix} \dot{q}_v \\ \{\dot{u}_b\} \end{Bmatrix}$$
$$+ \begin{bmatrix} k_v & -k_v\{N\}^{\mathrm{T}} \\ -k_v\{N\} & [k_b] + v^2m_v\{N\}\dfrac{\partial^2\{N\}^{\mathrm{T}}}{\partial x^2} + vc_v\{N\}\dfrac{\partial\{N\}^{\mathrm{T}}}{\partial x} + k_v\{N\}\{N\}^{\mathrm{T}} \end{bmatrix} \begin{Bmatrix} q_v \\ \{u_b\} \end{Bmatrix} = \begin{Bmatrix} 0 \\ -m_vg\{N\}_c \end{Bmatrix}, \tag{18}$$

where $\{u_b\}$ denotes the displacement vector of the bridge element, and $[m_b]$, $[c_b]$ and $[k_b]$ denote the mass, damping and stiffness matrices of the bridge element, $\{N\}$ is a vector containing cubic Hermitian interpolation functions associated with the transverse displacement of the element, and $\{N\}_c$ represents the vector $\{N\}$ evaluated at the co-ordinate position of the contact point of the sprung mass.

By a condensation procedure, the vehicle displacement q_v in Eq. (18) can be condensed into the displacement vector $\{u_b\}$ of the element in contact, resulting in the so-called VBI element [19]. The VBI element so derived can then be assembled with equations of other bridge elements not directly

in contact with the sprung mass to yield the system equations as

$$[M]\{\ddot{q}\} + [C]\{\dot{q}\} + [K]\{q\} = \{F\}, \tag{19}$$

where $\{q\}$ denotes the system displacement vector, which contains all the bridge degrees of freedom, $\{F\}$ the corresponding force vector, and $[M]$, $[C]$, $[K]$ the mass, damping and stiffness matrices of the system assembled from those of the VBI element and non-contact bridge elements. Apparently, all the system matrices and vectors are functions of the acting position of the sprung mass, which therefore are time-dependent.

The system equations as given in Eq. (19) can be solved by the Newmark β method of direct integration [20]. Consider a typical time step from t to $t + \Delta t$ in the non-linear time–history. The acceleration and velocity vectors of the system at $t + \Delta t$ can be discretized as follows:

$$\{\ddot{q}\}_{t+\Delta t} = a_0(\{q\}_{t+\Delta t} - \{q\}_t) - a_2\{\dot{q}\}_t - a_3\{\ddot{q}\}_t, \tag{20}$$

$$\{\dot{q}\}_{t+\Delta t} = \{\dot{q}\}_t + a_6\{\ddot{q}\}_t + a_7\{\ddot{q}\}_{t+\Delta t}, \tag{21}$$

where the coefficients are

$$\begin{aligned} &a_0 = \frac{1}{\beta\Delta t^2}, \qquad a_1 = \frac{\gamma}{\beta\Delta t}, \qquad a_2 = \frac{1}{\beta\Delta t}, \qquad a_3 = \frac{1}{2\beta} - 1, \\ &a_4 = \frac{\gamma}{\beta} - 1, \quad a_5 = \frac{\Delta t}{2}\left(\frac{\gamma}{\beta} - 2\right), \quad a_6 = \Delta t(1-\gamma), \qquad a_7 = \gamma\Delta t. \end{aligned} \tag{22}$$

In this study, $\beta = 0.25$ and $\gamma = 0.5$ are selected, which implies a constant average acceleration with unconditional numerical stability.

Substituting Eqs. (20) and (21) into the system Eq. (19), one can obtain after some manipulations the following equivalent linear equations:

$$[\bar{K}]_t\{q\}_{t+\Delta t} = \{\bar{F}\}_{t+\Delta t}, \tag{23}$$

where $[\bar{K}]$ represents the effective stiffness matrix and $\{\bar{F}\}$ the effective load vector, defined as follows:

$$[\bar{K}]_t = [K]_t + a_0[M]_t + a_1[C]_t, \tag{24}$$

$$\{\bar{F}\}_{t+\Delta t} = \{F\}_{t+\Delta t} + [M]_t(a_0\{q\}_t + a_2\{\dot{q}\}_t + a_3\{\ddot{q}\}_t), \tag{25}$$

where $[K]_t$, $[M]_t$ and $[C]_t$ are, respectively, the stiffness, mass and damping matrices of the system evaluated at time t. The force vector $\{F\}_{t+\Delta t}$ denotes the external loads of the system at time $t + \Delta t$.

For a vehicle with an assumed speed v, the philosophy for solving the system Eq. (19) at each time step, i.e., at time $t + \Delta t$, is as follows: (1) Use the system matrices $[M]_t$, $[C]_t$, $[K]_t$ at time step t to compute the effective stiffness matrix $[\bar{K}]_t$. (2) Calculate the acting position x_c of the sprung mass. (3) Calculate the external force vector $\{F\}_{t+\Delta t}$ and the effective load vector $\{\bar{F}\}_{t+\Delta t}$. (4) Solve the equivalent system Eq. (23) for the displacements $\{q\}_{t+\Delta t}$. (5) Compute the system accelerations and velocities from Eqs. (20) and (21). (6) Update the system matrices $[M]_t$, $[C]_t$, $[K]_t$ for the next time step. (7) Repeat steps (1)–(6).

6. Verification of accuracy of analytical solutions

In this section, the accuracy of the single-mode closed-form solution obtained for the VBI system, in particular, the vehicle response, will be verified by the finite element solution for a typical example. Consider a simply supported beam of length $L = 25\,\text{m}$, with the following properties: cross-sectional area $A = 2.0\,\text{m}^2$, moment of inertia $I = 0.12\,\text{m}^4$, mass per unit length $m = 4800\,\text{kg/m}$, and elastic modulus $E = 27.5\,\text{GN/m}^2$. The following data are adopted for the vehicle: mass $m_v = 1200\,\text{kg}$, spring stiffness $k_v = 500\,\text{kN/m}$, and zero damping. For this example, the vehicle to bridge mass ratio is 1/100. In the finite element analysis, 10 beam elements are used for the bridge. The fundamental vibration frequency of bridge is $\omega_b = 2.08\,\text{Hz}$ and the vehicle frequency is $\omega_v = 3.25\,\text{Hz}$.

For the case where the vehicle passes through the beam at a speed of $v = 10\,\text{m/s}$, the vertical displacements of the vehicle and the bridge midpoint obtained by the two approaches have been plotted in Figs. 9(a) and (b), respectively. As can be seen from Fig. 9(b), the solutions obtained by the two approaches show high degree of coincidence for the bridge response. Although slight deviations exist between the two solutions obtained for the vehicle response, the analytical results are considered acceptable for the purpose of *identifying* the key parameters involved.

The vertical velocity responses of the sprung mass and the midpoint of the beam are shown in Figs. 10(a) and (b), respectively, and the acceleration responses in Figs. 11(a) and (b). As can be seen, generally accurate solutions have been obtained for all cases by the single-mode analytical approach, except for the midpoint bridge acceleration, where drastic oscillations due to higher modes were missing, compared with the finite element solution. Aside from the higher modes, both approaches reveal similar trends for the fundamental mode concerning the midpoint bridge acceleration.

A general conclusion from the results shown in Figs. 9–11 is that the single-mode analytical solutions can be reliably used to simulate both the vehicle and bridge responses, except the midpoint acceleration of the bridge. Since the primary goal of this paper is to *conceptually* develop a technique for extracting the *fundamental* frequency of the bridge from the *vehicle response*, rather than from the bridge response, the inherent lack of capability of the single-mode approach to deal with the higher modes of the bridge is not considered a handicap.

7. Extraction of fundamental frequency of bridge

In this section, we shall try to extract the fundamental frequency of the bridge from the time-history vertical vibration response of the vehicle obtained by the finite element method, which is more "realistic" than the analytical one due to inclusion of the high-mode effects. Again, the idea is to demonstrate that the bridge frequency can be successfully extracted from the "simulated" vehicle response, before we go for the field test and extract the bridge frequency from the "recorded" response of a moving vehicle (that can be modelled as a sprung mass) during its passage over a real bridge.

The frequency responses for the vertical acceleration of the vehicle and the bridge midpoint have been plotted in Figs. 12(a) and (b), respectively, in which the fundamental frequency of the bridge is indicated by a vertical dashed line. Zero damping is assumed for the bridge. As can be

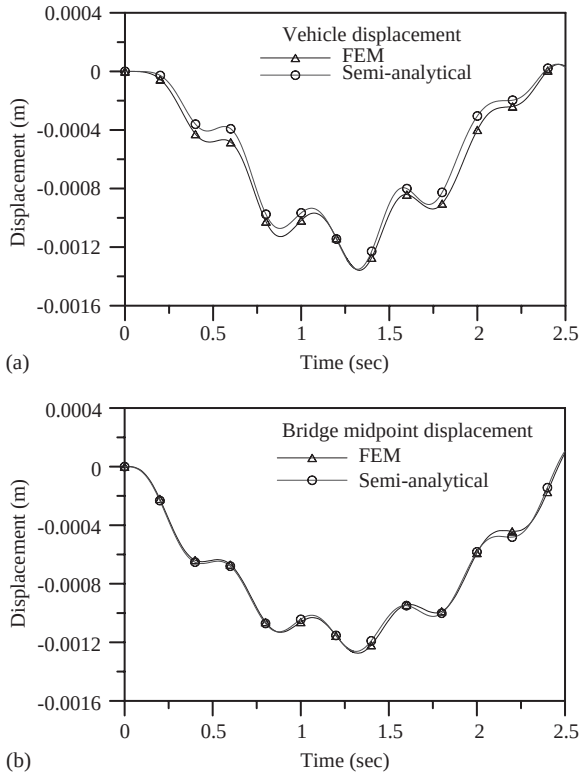

Fig. 9. Vertical displacement response of (a) vehicle and (b) bridge midpoint ($v = 10$ m/s).

seen, both the single-mode and finite element approaches yield almost identical results, except that the high-mode frequency contents were missing from the bridge response. Of interest is the fact that half the driving frequency of the vehicle, $\pi v/L (= 0.2$ Hz), can be observed as the lowest peak in the bridge spectrum shown in Fig. 12(b).

From the vehicle acceleration spectrum shown in Fig. 12(a), one observes that the four system frequencies dominating the vehicle response, i.e., $2\pi v/L$, $\omega_b - \pi v/L$, $\omega_b + \pi v/L$ and ω_v, or 0.4, 1.88, 2.08 and 3.24 Hz, appear as local peaks. Evidently, the bridge frequency ω_b is contained in the vehicle response, but *shifted* by an amount $\pi v/L$ due to the vehicle movement. It should be noted that the case presented herein belongs to the non-resonant case discussed in Section 4. In the following, some parametric studies will be conducted concerning the extraction of bridge frequencies.

7.1. Effect of moving speed of the vehicle

The frequency responses of the vehicle acceleration computed for various vehicle speeds using the single-mode approach and finite element approach have been plotted in Fig. 13(a) and (b), respectively. As can be seen from part (a), the three system frequencies $2\pi v/L$, $\omega_b - \pi v/L$ and $\omega_b + \pi v/L$ shift continuously as the vehicle speed v increases. The same shifting phenomenon can

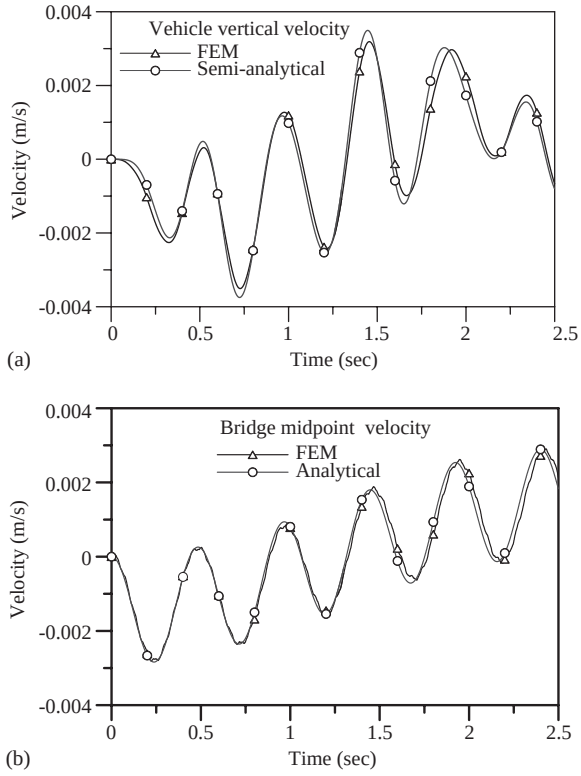

Fig. 10. Vertical velocity response of (a) vehicle and (b) bridge midpoint ($v = 10$ m/s).

be observed from the finite element results shown in part (b). The highest peak in each curve (i.e., for one specific speed) in part (b) represents the frequency of the bridge, but with a plus shift of $\pi v/L$. Such an effect should be taken into account in extracting the bridge frequency from the vehicle response. Moreover, the magnitude of the peak associated with the bridge frequency increases as the vehicle speed increases, which means that, from the point of field measurement, higher visibility can be achieved if the vehicle is allowed to move at a faster speed.

7.2. Condition of resonance

Because the fundamental frequency of the bridge contained in the vehicle response shifts as the vehicle speed v increases, there is a possibility for the occurrence of resonance if the shifted frequency $\omega_b + \pi v/L$ becomes equal or close to the vehicle frequency ω_v, as described in Section 4. To investigate such an effect, we adjust the vehicle suspension stiffness k_v to 296 kN/m, which implies a vehicle frequency of $\omega_v = 2.50$ Hz. If the vehicle speed is selected as 20 m/s(= 72 km/h), then the shifted frequency $\omega_b + \pi v/L$ is 2.48 Hz, which is quite close to the vehicle frequency ω_v. The vertical acceleration of the vehicle obtained for $v = 20$ m/s by the finite element approach has been plotted in Fig. 14, together with the response for a reference speed of $v = 10$ m/s. Clearly,

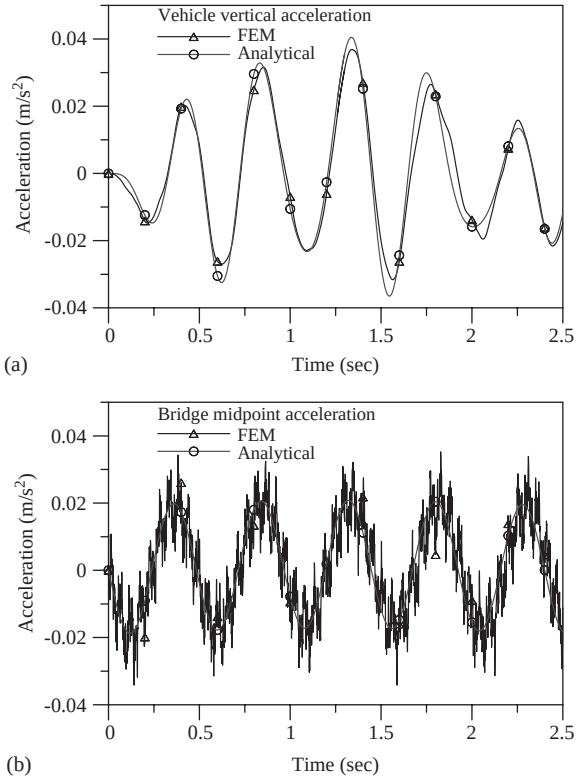

Fig. 11. Vertical acceleration response of (a) vehicle and (b) bridge midpoint ($v = 10$ m/s).

resonance is excited on the vehicle when it moves at $v = 20$ m/s, as the response increases following the movement of the vehicle. In contrast, the case with $v = 10$ m/s should be regarded as a non-resonant case. From the frequency response plot given in Fig. 15, one observes that higher visibility exists for the bridge frequency ω_b under the resonance condition (i.e. with $v = 20$ m/s). Of interest is the fact that for the non-resonant case (i.e. $v = 10$ m/s), the bridge frequency remains visible and can be clearly identified. This is the case commonly encountered in practice.

For the present interest, the vertical response of the bridge midpoint under the same speed $v = 20$ m/s was plotted in Fig. 16, together with that for $v = 10$ m/s. Clearly, no resonance exists for the bridge at the speed $v = 20$ m/s. Such a result is not surprising, if one realizes that the kinetic energy of the bridge (a larger subsystem) is dissipated by the vehicle (a smaller subsystem) in the form of resonance, as the latter plays the role of a "tuned mass".

As a side note, if the first resonance condition mentioned in Section 4, i.e., $S = 1$, is to be met for the present case, the vehicle has to move at a speed of $v = 104$ m/s = 374 km/h, which can hardly be reached in practice. On the other hand, if use is to be made of the second resonance condition, i.e., $\omega_v^2 - (2\pi v/L)^2 = 0$ or $\omega_v - 2\pi v/L = 0$, then the vehicle has to move at a speed of $v = 62.5$ m/s = 225 km/h, which is still too high to be adopted in a field test.

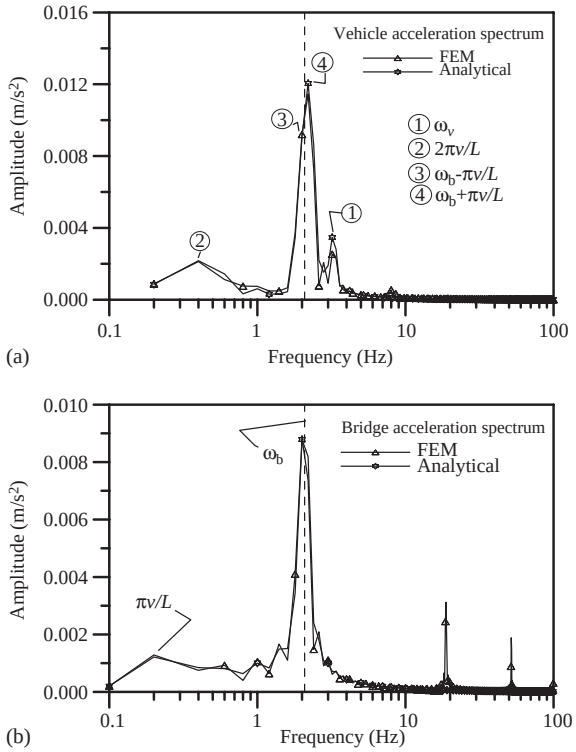

Fig. 12. Vertical acceleration spectrum of (a) vehicle and (b) bridge midpoint ($v = 10$ m/s).

7.3. Effect of damping of the bridge

To investigate the effect of damping of bridge on the vehicle response, three values of damping ratio are considered for the bridge, i.e. 0%, 2% and 5%. The other data are the same as those used in Section 6. From the result plotted in Fig. 17, it is certain that the visibility of the bridge frequency decreases due to the presence of damping. Nevertheless, it can still be identified from the vehicle acceleration spectrum with no difficulty.

7.4. Effect of vehicle traveling over a stiffer bridge

In practice, a well-designed bridge is so arranged that it cannot be easily excited by vehicles traveling at "normal" speeds. This is why in some design codes, the fundamental frequency of the highway bridge is recommended to lie outside of the vehicle frequencies ranging between 2 and 5 Hz. To reflect such a situation, we have chosen to increase the stiffness of the bridge studied in Section to a value of $EI = 11.25\,\mathrm{GN\,m^2}$, while keeping all the other data unchanged. The first frequency of the bridge is $\omega_b = 5.44$ Hz, which is much greater than the vehicle frequency $\omega_v = 3.25$ Hz. For the vehicle traveling with speed $v = 10$ m/s, no resonance will be excited on the bridge. From the vehicle acceleration spectrum plotted in Fig. 18, it is

confirmed that even for such a non-resonant case, the bridge frequency can be extracted with no difficulty, though there is a substantial drop in the peak response compared with the previous cases.

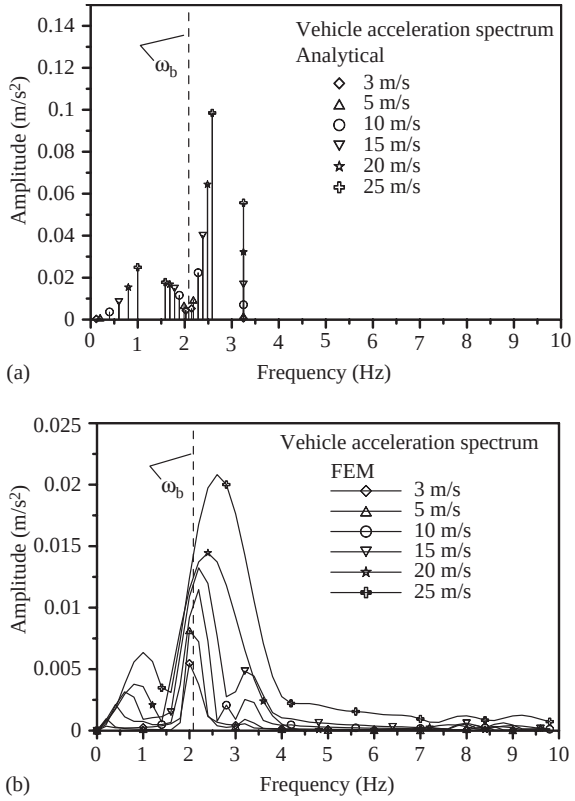

Fig. 13. Vertical acceleration spectrum of vehicle: (a) analytical and (b) FEM.

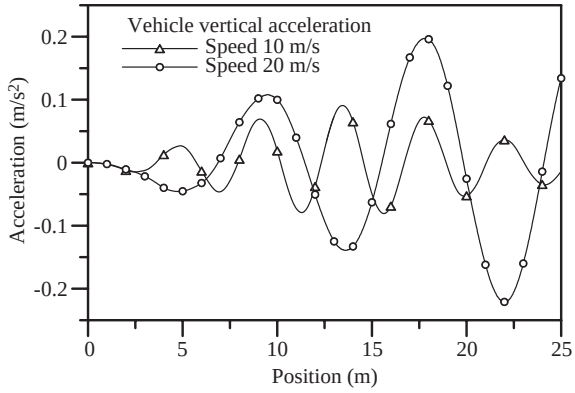

Fig. 14. Vertical acceleration response of vehicle (resonant case).

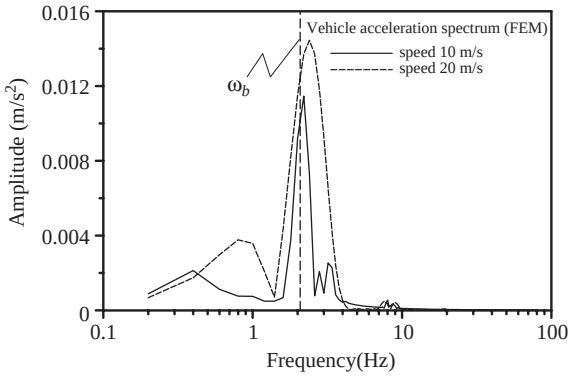

Fig. 15. Vertical acceleration spectrum of vehicle (resonant case).

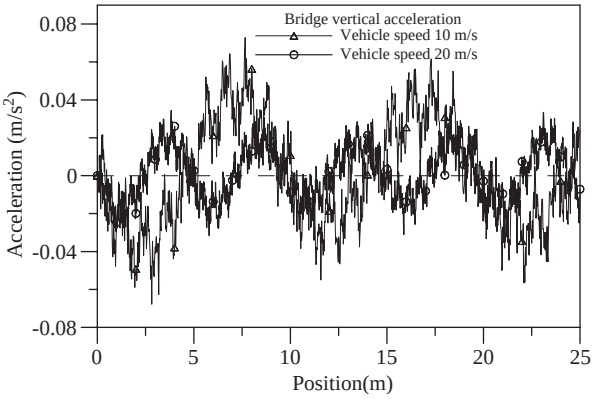

Fig. 16. Vertical acceleration response of bridge (resonant case).

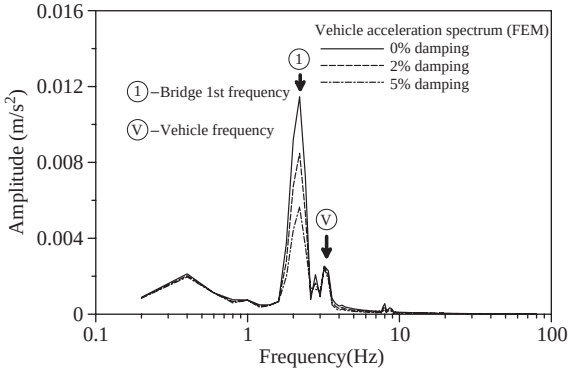

Fig. 17. Effect of damping of bridge.

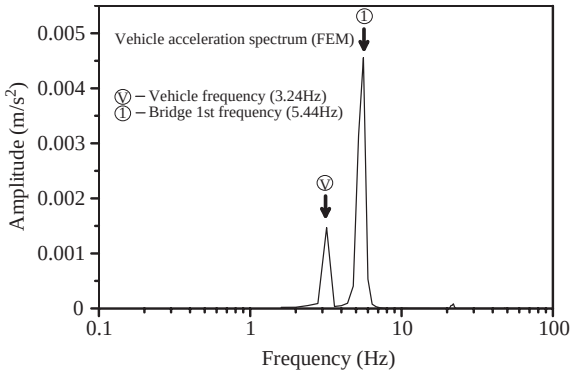

Fig. 18. Acceleration spectrum for vehicle traveling over a stiffer bridge.

8. Concluding remarks

This paper represents a preliminary study on the feasibility of extracting the fundamental bridge frequency from the dynamic response of a vehicle passing over the bridge. As a first attempt to identify the key parameters dominating the VBI response, some assumptions that lead to closed-solution, are adopted. The results obtained from the single-mode approach have been verified to be quite accurate by an independent finite element analysis, which does not rely on any particular assumptions. From both the analytical and finite element studies, it is ascertained that the bridge frequency is contained in and can be extracted from the vehicle acceleration spectrum, but a correction must be made for the shifting effect. Higher vehicle speeds can result in higher amplitudes for the bridge frequency, which implied higher visibility and therefore is good for signal processing. The resonance condition for the moving vehicle to achieve the maximum response was discussed in details, which, though, may not be encountered in practice. Noteworthy is the fact that the visibility of the bridge frequencies remains good even for non-resonant case or in the presence of bridge damping.

Future research should be conducted to address the factors not covered in this preliminary study, including in particular the engine vibrations, pitching and rolling motions, damping and suspension mechanisms of the vehicle, pavement roughness, multi-span effect, multi-lane effect of the bridge, existing traffic effect, and so on.

Acknowledgements

The research reported herein is sponsored in part by the National Science Council of the Republic of China through grant nos. NSC 89-2211-E-002-113 and NSC 90-2211-E-002-057.

References

[1] V.R. McLamore, G.C. Hart, I.R. Stubbs, Ambient vibration of two suspension bridges, *Journal of the Structural Division, American Society of Civil Engineers* 97 (ST10) (1971) 2567–2582.

[2] A.M. Abdel-Ghaffar, G.W. Housner, Ambient vibration tests of suspension bridge, *Journal of the Engineering Mechanics Division, American Society of Civil Engineers* 104 (EM5) (1978) 983–999.
[3] D.F. Mazurek, J.T. DeWolf, Experimental study of bridge monitoring technique, *Journal of Structural Engineering, American Society of Civil Engineers* 116 (9) (1990) 2532–2549.
[4] J.R. Casas, Full-scale dynamic testing of the Alamillo cable-stayed bridge in Sevilla (Spain), *Earthquake Engineering and Structural Dynamics* 24 (1995) 35–51.
[5] P. Paultre, J. Proulx, M. Talbot, Dynamic testing procedures for highway bridges using traffic loads, *Journal of Structural Engineering, American Society of Civil Engineers* 121 (2) (1995) 362–376.
[6] C.E. Ventura, A.J. Felber, S.F. Stiemer, Determination of the dynamic characteristics of the Colquitz River Bridge by full-scale testing, *Canadian Journal of Civil Engineering* 23 (1996) 536–548.
[7] G.H. Conner, J.M. Stallings, T.L. McDuffie, J.R. Campbell, R.Y. Fulton, B.A. Shelton, R.B. Mullins, Steel bridge testing in Alabama, *Transportation Research Record* 1594 (1997) 134–139.
[8] C.R. Farrar, C.H. James III, System identification from ambient vibration measurements on a bridge, *Journal of Sound and Vibration* 205 (1) (1997) 1–18.
[9] Y. Fujino, M. Abe, H. Shibuya, M. Yanagihara, M. Sato, S. Nakamura, Y. Sakamoto, Forced and ambient vibration tests and vibration monitoring of Hakucho Suspension Bridge, *Transportation Research Record* 1696 (2) (2000) 57–63.
[10] C.C. Chang, T.Y.P. Chang, Q.W. Zhang, Ambient vibration of long-span cable-stayed bridge, *Journal of Bridge Engineering, American Society of Civil Engineers* 6 (1) (2001) 46–53.
[11] J.M.W. Brownjohn, M. Bocciolone, A. Curami, M. Falco, A. Zasso, Humber Bridge full-scale measurement campaigns 1990–1991, *Journal of Wind Engineering and Industrial Aerodynamics* 52 (1994) 185–218.
[12] Y.L. Xu, L.D. Zhu, K.Y. Wong, K.W.Y. Chan, Field measurement results of Tsing Ma Suspension Bridge during Typhoon Victor, *Structural Engineering and Mechanics* 10 (6) (2000) 545–559.
[13] B.M. Douglas, W.H. Reid, Dynamic tests and system identification of bridges, *Journal of the Structural Division, American Society of Civil Engineers* 108 (10) (1982) 2295–2312.
[14] C.S. Huang, Y.B. Yang, L.Y. Lu, C.H. Chen, Dynamic testing and system identification of a multi-span highway bridge, *Earthquake Engineering and Structural Dynamics* 28 (1999) 857–878.
[15] I. Okauchi, T. Miyata, M. Tatsumi, R. Kiyota, Dynamic field tests and studies on vibrational characteristics of long-span suspension bridges, *Structural Engineering/Earthquake Engineering, Japan Society of Civil Engineers* 9 (1) (1992) 89–100.
[16] E.M. Maragakis, B.M. Douglas, Q. Chen, U. Sandirasegaram, Full-scale tests of a railway bridge, *Transportation Research Record* 1624 (1998) 140–147.
[17] J.M. Biggs, *Introduction to Structural Dynamics*, McGraw-Hill, New York, NY, 1964 pp. 315–328.
[18] R.A. Dusseau, H.N. Dusaisi, Natural frequencies of concrete bridges in the Pacific Northwest, *Transportation Research Record* 1393 (1993) 119–132.
[19] Y.B. Yang, J.D. Yau, Vehicle-bridge interaction element for dynamic analysis, *Journal of Structural Engineering American Society of Civil Engineers* 123 (11) (1997) 1512–1518.
[20] N.M. Newmark, A method of computation for structural dynamics, *Journal of the Engineering Mechanics Division, American Society of Civil Engineers* 85 (EM3) (1959) 67–94.